Small-Angle Neutron Scattering from Mixtures of Sodium Dodecyl Sulfate and a Cationic, Bolaform Surfactant Containing Azobenzene

F. Pierce Hubbard, Jr.,† Gabriella Santonicola,‡ Eric W. Kaler,‡ and Nicholas L. Abbott*,†

Department of Chemical and Biological Engineering, University of Wisconsin-Madison, 1415 Engineering Drive, Madison, Wisconsin 53706-1691, and Center for Molecular and Engineering Thermodynamics, Department of Chemical Engineering, University of Delaware, Newark, Delaware 19716

Received January 29, 2005. In Final Form: April 22, 2005

This paper reports on the microstructures formed in aqueous solutions containing mixtures of sodium dodecyl sulfate (SDS) and a photosensitive, bolaform surfactant, bis(trimethylammoniumhexyloxy)-azobenzene dibromide (BTHA). By using quasi-elastic light scattering and small-angle neutron scattering, we determined that aqueous solutions containing SDS and the trans isomer of BTHA (0.1 wt % total surfactant, 15 mol % BTHA, 85 mol % SDS) form vesicles with average hydrodynamic diameters of 1350 ± 50 Å and bilayer thicknesses of 35 ± 2 Å. The measured bilayer thickness is consistent with a model of the vesicle bilayer in which the trans isomer of BTHA spans the bilayer. Upon illumination with UV light, the BTHA underwent photoisomerization to produce a cis-rich photostationary state (80% cis isomer). We measured this photoisomerization to drive the reorganization of vesicles into cylindrical aggregates with cross-sectional radii of 19 ± 3 Å and average hydrodynamic diameters of 240 ± 50 Å. Equilibration of the cis-rich solution in the dark at 25 °C for 12 h or illumination of the solution with visible light leads to the recovery of the trans-rich photostationary state of the solution and the reformation of vesicles, thus demonstrating the potential utility of this system as the basis of a tunable fluid.

Introduction

Materials that respond to stimuli such as heat, light, or electric fields are potentially useful in a broad range of technologies, including controlled delivery of drugs or fragrances,[1] molecular separations,[2] control of microscale systems,[3] and as tunable templates for directing the synthesis of higher order structures.[4,5] A vesicle formed by amphiphilic molecules represents a particularly interesting microstructure because it is possible to encapsulate an aqueous solution within the interior of a vesicle or to host sparingly water-soluble molecules within the shell of a vesicle.[6] In this paper, we report on aqueous dispersions of vesicles formed by mixtures of sodium dodecyl sulfate (SDS) and the light-sensitive, bolaform surfactant bis(trimethylammoniumhexyloxy)azobenzene dibromide (BTHA, Figure 1) and describe the use of small-angle neutron scattering (SANS) and quasi-elastic light scattering (QLS) to characterize the changes in microstructure that accompany the illumination of these solutions with ultraviolet and visible light.

The experimental system reported in this paper builds on past studies of aqueous mixtures of anionic and cationic surfactants that have been shown to form vesicular aggregates in solution.[7−11] Whereas mixtures of oppositely charged surfactants with equal or nearly equal chain lengths typically do not form vesicles at equilibrium (precipitates or lamellae are generally observed),[7,8] surfactant mixtures with dissimilar chain lengths, branched

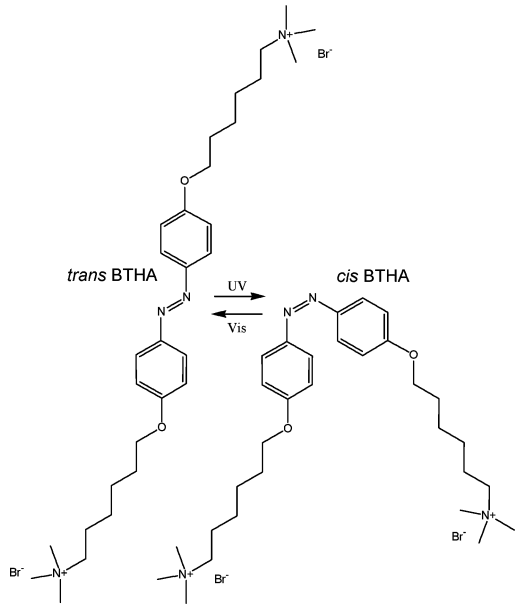

Figure 1. Structures of trans and cis isomers of BTHA.

* Corresponding author. E-mail: abbott@engr.wisc.edu. Phone: +1-608-265-5278. Fax: +1-608-262-5434.
† University of Wisconsin-Madison.
‡ University of Delaware.

(1) Fendler, J. *Membrane Mimetic Chemistry*; Wiley: New York, 1983.
(2) Rosslee, C. A.; Abbott, N. L. *Anal. Chem.* **2001**, *73*, 4808−4814.
(3) Gallardo, B. S.; Gupta, V. K.; Eagerton, F. D.; Jong, L. I.; Craig, V. S.; Shah, R. R.; Abbott, N. L. *Science* **1999**, *283*, 57−60.
(4) Hentze, H.-P.; Raghavan, S. R.; McKelvey, C. A.; Kaler, E. W. *Langmuir* **2003**, *19*, 1069−1074.
(5) Liu, S.; Gonzalez, Y. I.; Kaler, E. W. *Langmuir* **2003**, *19*, 10732−10738.
(6) Karukstis, K. K.; Zieleniuk, C. A.; Fox, M. J. *Langmuir* **2003**, *19*, 10054−10060.
(7) Herrington, K. L.; Kaler, E. W.; Miller, D. D.; Zasadzinski, J. A.; Chiruvolu, S. *J. Phys. Chem.* **1993**, *97*, 13792−13802.
(8) Wang, C.; Tang, S.; Huang, J.; Zhang, X.; Fu, H. *Colloid Polym. Sci.* **2002**, *280*, 770−774.
(9) Yan, Y.; Huang, J.; Li, Z.; Ma, J.; Fu, H.; Ye, J. *J. Phys. Chem. B* **2003**, *107*, 1479−1482.
(10) Iampietro, D.; Kaler, E. *Langmuir* **1999**, *15*, 8590−8601.
(11) Yatcilla, M.; Herrington, K.; Brasher, L.; Kaler, E. *J. Phys. Chem.* **1996**, *100*, 5874−5879.

10.1021/la050263c CCC: $30.25
Published on Web 06/11/2005

tails, or bulky counterions have been reported to spontaneously form vesicles.[7,9−11] For example, mixtures of cetyltrimethylammonium bromide (CTAB) and sodium octyl sulfate (SOS) form vesicles that are stable for many months with a size distribution that can be recovered after perturbation by heat or sonication.[12,13] These results support the proposition that vesicles are equilibrium microstructures in some mixed surfactant systems and that their size distribution is, thus, a thermodynamic property of the system. Other results, however, have been interpreted to contradict this proposition.[14] Whereas past studies have established that the molecular architectures of surfactants are important in determining whether vesicles form in mixed surfactant systems,[10−13,15−18] how a bolaform architecture influences the tendency of a surfactant to spontaneously form vesicular microstructures is not understood. We hypothesized that packing constraints imposed by the rigid, bolaform nature of BTHA would play a role in determining the types of microstructures formed in this system and that these same packing constraints would cause the photoisomerization of BTHA to trigger substantial changes in these microstructures.

We have previously reported that BTHA within aqueous mixtures of BTHA and SDS undergoes reversible isomerization to cis-rich photostationary states and/or trans-rich photstationary states upon illumination with UV light (335 nm) or visible light (440 nm), respectively.[19] We have also reported that illumination of this system leads to reversible changes in the dynamic interfacial behavior of aqueous systems of these surfactants as well as reversible changes in the scattering of light from bulk solutions.[19] In this paper, we characterize the microstructures of the aggregates formed by these surfactants by using SANS in combination with QLS. These studies demonstrate the existence of vesicular aggregates in these solutions as well as reversible changes between a vesicular and a cylindrical aggregate morphology upon illumination.

We conclude this introduction by noting that a number of other studies using azobenzene-containing surfactants as light-sensitive triggers have been reported, including studies that have reported the disruption of microemulsions and manipulation of equilibrium surface tensions of aqueous solutions.[20,21] In particular, we note that Sakai, Abe, and co-workers have interpreted transmission electron micrographs of mixtures of 4-butylazobenzene-4′-(oxyethyl)trimethylammonium bromide (AZTMA) and sodium dodecyl benzene sulfonate (SDBS) to indicate formation of vesicles in multiphase systems.[22] Our work complements this past study by examining an azobenzene-based surfactant that has a bolaform architecture and by performing SANS to characterize the microstructure of the surfactant system.

Experimental Section

Materials. All reagents were obtained from Aldrich (Milwaukee, WI). SDS was recrystallized three times in ethanol prior to use. BTHA was synthesized as previously described and recrystallized three times in ethanol prior to use.[19] D_2O (99.9% deuteration) was obtained from Cambridge Isotope Laboratories (Andover, MA).

Methods. Stock solutions of either BTHA or SDS were prepared by weighing the appropriate mass of surfactant into a scintillation vial and then adding deionized and distilled H_2O (18.2 MΩ·cm, Millipore) or D_2O. Surfactant mixtures were prepared by mixing stock solutions filtered through a 0.22-μm Millex-GV filter. *trans*-BTHA solutions were illuminated using a Spectroline E-Series lamp with a filter (model EN280L, Westbury, NY) to produce a solution enriched with the cis isomer. The lamp emitted light with wavelengths from 300 to 450 nm, with a peak intensity at 365 nm. The filter was designed to eliminate light with wavelengths greater than 410 nm. Unless stated otherwise, all solutions reported in this study were illuminated in borosilicate test tubes with diameters of 12 mm (Fisher, Atlanta, GA). Samples prepared for SANS were illuminated in quartz cells (see below) provided by the National Institute of Standards and Technology (NIST).

Prior to performing QLS and SANS experiments, the time required for a solution containing 0.1 wt % total surfactant (15 mol % BTHA/85 mol % SDS) to reach the photostationary state under illumination with UV light was determined. Following illumination of the mixture of BTHA and SDS with UV light, the optical absorption spectrum of the mixture was recorded using a Cary 1E UV−vis spectrophotometer (Varian, Walnut Creek, CA). UV−vis spectra of solutions containing mixtures of BTHA and SDS have been reported previously,[19] and the photostationary state was determined to have been reached when the UV−vis spectra of the solution did not change with further illumination (5 min for a solution containing 0.1 wt % total surfactant comprised of 15 mol % BTHA and 85 mol % SDS).

QLS. QLS measurements were conducted using a Brookhaven light scattering apparatus (Brookhaven Instruments, Holtsville, NY), comprised of a BI-9000AT digital autocorrelator, BI-200SM goniometer, and 100-mW laser (532 nm, Coherent Compass 315M-100). The detector angle was set to 90°, and the autocorrelation curves were analyzed using the method of cumulants.[23] This method provides the average decay rate, $\langle\tau\rangle = \langle D_T\rangle q^2$, where $\langle D_T\rangle$ is the average translational diffusion coefficient and q is the magnitude of the scattering vector. The normalized, relative variance is calculated as $v = (\langle\tau^2\rangle - \langle\tau\rangle^2)/\langle\tau\rangle^2$. $\langle D_T\rangle$ is related to the hydrodynamic diameter according to the Stokes−Einstein equation.[24]

SANS. SANS measurements were performed using the NG3 instrument at NIST in Gaithersburg, MD. The wavelengths of the neutrons were on average 6 Å, with a spread in wavelength, $\Delta\lambda/\lambda$, of 14%. Data were collected with the detector set at three positions: 1.33, 4.5, and 13 m from the sample. By offsetting the detector 25 cm from center, these distances covered q ranges of 0.04−0.4, 0.008−0.1, and 0.004−0.04 Å^{-1}, respectively. Samples were held in quartz cells with a path length of 5.0 mm and placed in a sample chamber thermostated at 25.0 ± 0.1 °C. To ensure good statistics, at least 10^6 detector counts were collected for each sample at each distance. The data were corrected for detector efficiency, background radiation, empty cell scattering, and incoherent scattering to calculate the scattered intensity on an absolute scale. These procedures were performed using a computer program provided by NIST that runs on IGOR Pro (Wavemetrics, Lake Owego, Oregon).

We used Guinier analysis, form factor modeling, and the indirect Fourier transform (IFT) technique to interpret the SANS spectra. All of these techniques have been discussed extensively in the literature[25−31] and are only summarized here. For samples identified by Guinier analysis to contain vesicles, we fit the data using a polydisperse core−shell model, in which the vesicles have a polydisperse core radius and a constant shell thickness, to the experimental data. The distribution of vesicle sizes was modeled

(12) Jung, H. T.; Lee, S. Y.; Kaler, E. W.; Coldren, B.; Zasadzinski, J. A. *Proc. Natl. Acad. Sci. U.S.A.* **2002**, *99*, 15318−15322.
(13) Jung, H. T.; Coldren, B.; Zasadzinski, J. A.; Iampietro, D. J.; Kaler, E. W. *Proc. Natl. Acad. Sci. U.S.A.* **2001**, *98*, 1353−1357.
(14) Almgren, M.; Rangelov, S. *Langmuir* **2004**, *20*, 6611−6618.
(15) Kaler, E. W.; Murthy, A. K.; Rodriguez, B. E.; Zasadzinski, J. A. N. *Science* **1989**, *254*, 1371−1374.
(16) Kaler, E. W.; Herrington, K. L.; Murthy, K.; Zasadzinski, J. A. N. *J. Phys. Chem.* **1992**, *96*, 6698−6707.
(17) Yuet, P. K.; Blankschtein, D. *Langmuir* **1996**, *12*, 3802−3818.
(18) Yuet, P. K.; Blankschtein, D. *Langmuir* **1996**, *12*, 3819−3827.
(19) Shin, J.; Abbott, N. L. *Langmuir* **1999**, *15*, 4404−4410.
(20) Eastoe, J.; Dominguez, M. S.; Cumber, H.; Wyatt, P.; Heenan, R. K. *Langmuir* **2004**, *20*, 1120−1125.
(21) Shang, T.; Smith, K. A.; Hatton, T. A. *Langmuir* **2003**, *19*, 10764−10773.
(22) Sakai, H.; Matsumura, A.; Yokoyama, S.; Saji, T.; Abe, M. *J. Phys. Chem. B* **1999**, *103*, 10737−10740.
(23) Koppel, D. E. *J. Chem. Phys.* **1972**, *57*, 4814−4820.
(24) Hiemenz, P. C.; Rajagopalan, R. *Principles of Colloid and Surface Chemistry*, 3rd ed.; Marcel Dekker: New York, 1997.

as a Schultz distribution.[29] All samples were fit using the IFT technique. In this technique, the intensity of neutrons scattered from an isotropic sample, $I(q)$, can be expressed in terms of a form factor $P(q)$ and structure factor $S(q)$ as

$$I(q) = n_p P(q)\, S(q) \tag{1}$$

where n_p is the number density of scatterers. Under conditions of low q ($qR_g < 1$, where R_g is the radius of gyration) and dilute solution [$S(q) = 1$], Guinier analysis relates $I(q)$ to $P(q)$ for various geometries as[25,28]

spheres

$$P(q) = \left(\frac{\Delta\rho}{V}\right)^2 e^{-q^2R_g^2/3} \tag{2}$$

cylinders

$$P(q) = L\frac{\pi}{q}(\Delta\rho)^2A^2e^{-q^2R_c^2/2} \tag{3}$$

bilayers

$$P(q) = A\frac{2\pi}{q^2}(\Delta\rho)^2t^2e^{-q^2R_t^2} \tag{4}$$

where $\Delta\rho$ is the difference in scattering length density between the particle and the solvent. The symbols V, L, A, and t represent the volume of a sphere, length of a cylinder, cross-sectional area of a cylinder or total area of a vesicle shell, and thickness of a bilayer, respectively. The R_x's are radii of gyration, which can be related to quantities of interest such as sphere radii, cylinder cross-sectional radii, and bilayer thicknesses. The above expressions lead to the prediction that a plot of $\ln[I(q)]$ versus $\ln(q)$ should be linear with slopes of -1 and -2 for cylindrical and bilayer aggregates, respectively, when $qR_x < 1$.

The IFT technique permits evaluation of the pair distance distribution function or $p(r)$ from $I(q)$ by using the relation[30,31]

$$I(q) = 4\pi\int_0^\infty p(r)\frac{\sin(qr)}{qr}\,dr \tag{5}$$

Under conditions where $S(q) = 1$ and the population of scatterers is monodisperse, $p(r)$ evaluated by the IFT technique permits direct identification of the particle structure. We performed the IFT analysis using software provided by Glatter.[30,31] The only input parameter required by the IFT program is an estimate of D_{max}, corresponding to the value of r for which $p(r) = 0$ for $r > D_{max}$. For our evaluations, we selected D_{max} to be greater than the hydrodynamic size observed from QLS. Examples of $p(r)$ for various aggregate geometries have been reported in the literature, and three examples, which are used later in this paper to interpret our results, are shown in Figure 2.[10,32] Inspection of Figure 2 reveals that spheres, cylinders, and vesicles possess distinctly different $p(r)$ functions, thus, providing a way to distinguish between aggregate structures. With knowledge of aggregate shape, IFT is capable of aggregate-specific transforms that provide a more accurate determination of parameters of interest such as the radius of an aggregate with a cylindrical cross section or the thickness of a bilayer of a vesicle.[10,32]

Results and Discussion

Past studies of systems containing mixtures of cationic and anionic surfactants generally have shown that phase diagrams measured in H_2O differ from those measured in D_2O, due to an increased strength of hydrogen bonding in D_2O.[16,25,33] Because SANS requires the use of D_2O, we first addressed the influence of D_2O on the aggregation behavior of BTHA and SDS. For CTAB/SOS and CTAT/SDBS mixtures, phase diagrams measured at 25 °C in H_2O were similar to phase diagrams measured at 40 °C in D_2O.[16,25] For azobenzene molecules and derivatives, the trans isomer is the lowest energy state, and cis-rich solutions thermally relax to trans solutions in the absence of illumination (see below for discussion regarding dynamics). Hence, for the BTHA/SDS system, heating is undesirable because it increases the rate of thermal relaxation of the cis isomer back to the trans isomer. Thus, we report in this paper characterization of microstructures formed in D_2O and H_2O at 25 °C.

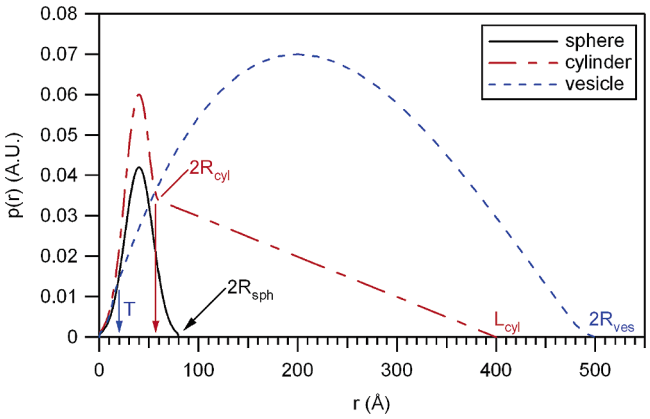

Figure 2. Calculated $p(r)$ functions for three different aggregate geometries. Symbols: T is the bilayer thickness of a vesicle, R_{ves} is the vesicle radius, R_{cyl} is the cylinder cross-sectional radius, L_{cyl} is the cylinder length, and R_{sph} is the sphere diameter.

Table 1. QLS Results for Trans, Cis-Rich, and *TCT* Samples[a]

sample	solvent	age	hydrodynamic diameter (Å)	relative variance
trans	D_2O	1 day	1350 ± 50	0.13 ± 0.1
	D_2O	2 day	1460 ± 50	0.12 ± 0.1
	H_2O	1 day	1290 ± 50	0.11 ± 0.1
	H_2O	2 day	1340 ± 50	0.10 ± 0.1
TCT	D_2O	1 day	1330 ± 50	0.13 ± 0.1
	D_2O	2 day	1430 ± 50	0.09 ± 0.1
	H_2O	1 day	1230 ± 50	0.10 ± 0.1
	H_2O	2 day	1280 ± 50	0.09 ± 0.1
cis	D_2O	5 min	240 ± 50	0.15 ± 0.1

[a] Hydrodynamic size is the average aggregate diameter obtained using cumulant analysis. Values reported here are the averages of three independent samples.

Trans Sample. We first prepared solutions containing 0.1 wt % total surfactant that comprised 15 mol % BTHA and 85 mol % SDS in D_2O and characterized these solutions using UV−vis spectroscopy after incubation at 25 °C for 2 h in the dark. These solutions were determined to contain 100% of the trans isomer of BTHA. Trans solutions appear pale yellow and scatter light strongly when illuminated with a laser. The solutions are not viscous. Because of the visible absorbance of the trans isomer of BTHA, it was not possible to observe the blue hue that has been reported in the past when vesicles are formed in solution from mixtures of cationic and anionic surfactants.[11]

We characterized these solutions by using QLS. As summarized in Table 1, after 1 day of equilibration, the average hydrodynamic diameter of aggregates in samples

(25) Brasher, L.; Kaler, E. *Langmuir* **1996**, *12*, 6270−6276.
(26) Hassan, P. A.; Fritz, G.; Kaler, E. W. *J. Colloid Interface Sci.* **2003**, *257*, 154−162.
(27) Porod, G. In *Small Angle X-ray Scattering*; Glatter, O., Kratky, O., Eds.; Academic Press: London, 1982.
(28) Guinier, A.; Fournet, G. *Small Angle Scattering of X-Rays*; John Wiley & Sons: New York, 1955.
(29) Gonzalez, Y. I.; Stjerndahl, M.; Danino, D.; Kaler, E. W. *Langmuir* **2004**, *20*, 7053−7063.
(30) Glatter, O. *J. Appl. Crystallogr.* **1977**, *10*, 415−421.
(31) Fritz, G.; Bergmann, A.; Glatter, O. *J. Chem. Phys.* **2000**, *113*, 9733−9740.
(32) Iampietro, D. J.; Brasher, L. L.; Kaler, E. W. *J. Phys. Chem. B* **1998**, *102*, 3105−3113.
(33) Chang, N. J.; Kaler, E. W. *J. Phys. Chem.* **1985**, *89*, 2996.

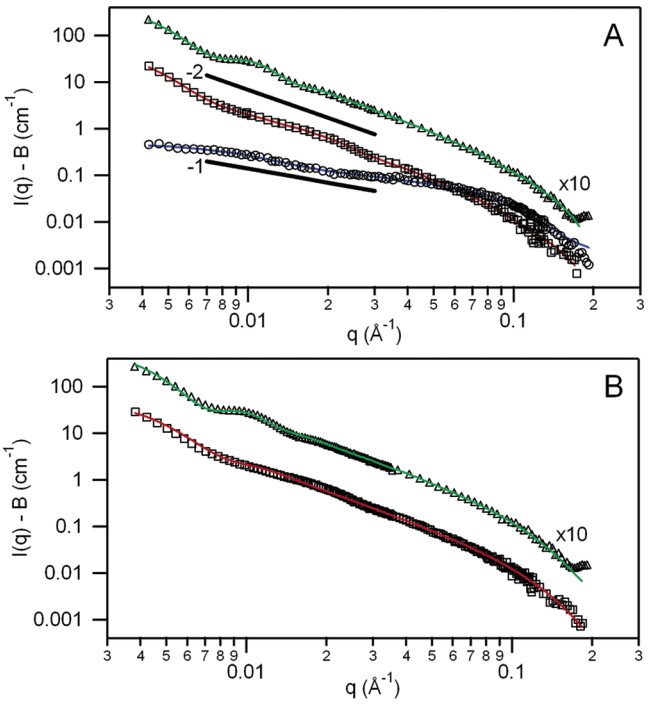

Figure 3. (A) SANS from D_2O solutions containing 0.1 wt % total surfactant (15 mol % BTHA/85 mol % SDS). Open symbols represent the data, and the solid lines indicate fits of the data using IFT with $S(q) = 1$. Trans (□), cis-rich (○), and *TCT* sample (△), which is scaled by a factor of 10 for clarity. (B) SANS data replotted with fits using a polydisperse core−shell model. Trans (□) and *TCT* sample (△), which is scaled by a factor of 10 for clarity.

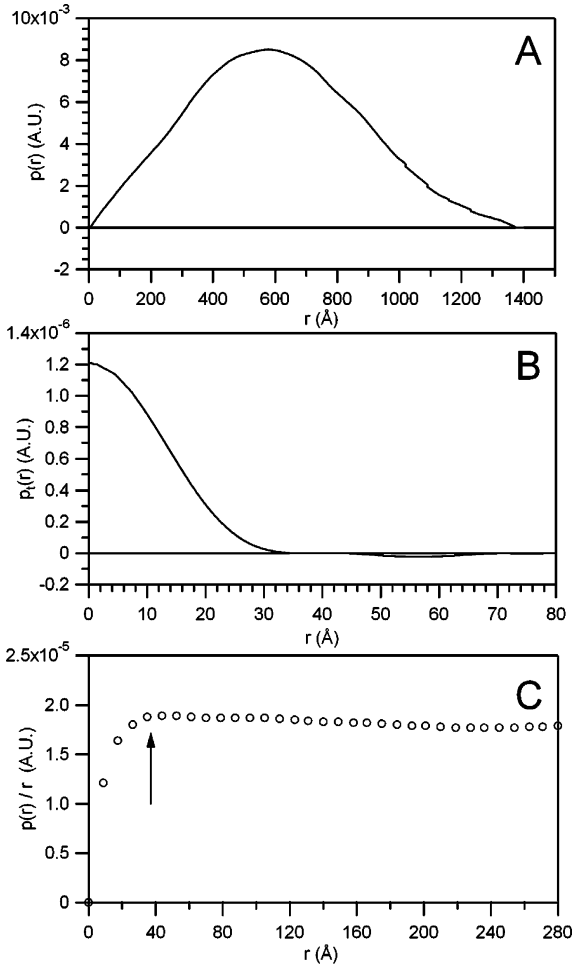

Figure 4. (A) Pair distance distribution function, $p(r)$, and (B) the thickness pair distance distribution function, $p_t(r)$, obtained by IFT analysis of the *trans*-BTHA/SDS sample shown in Figure 3A. (C) Plot of $p(r)/r$ vs r for the *trans*-BTHA/SDS sample. The arrow marks the crossover in the $p(r)$ from r^2 to linear dependence.

of *trans*-BTHA and SDS in D_2O was 1350 ± 50 Å. After one additional day of equilibration, their size had increased to 1460 ± 50 Å, indicating that these samples are not yet at equilibrium. As also shown in Table 1, the aggregate size measured in H_2O is marginally smaller than that measured in D_2O, suggesting that the increased strength of hydrogen bonding in D_2O has little effect on the aggregate size at this composition. Finally, we note that the hydrodynamic sizes reported in Table 1 are similar to those reported in H_2O in a previous study (1500 ± 100 Å, in 0.05 wt % total surfactant, 6 mol % BTHA/94 mol % SDS).[19]

We next performed SANS measurements to determine the microstructure of the aggregates containing *trans*-BTHA. Figure 3A shows the SANS data and corresponding IFT fit of the trans sample containing 0.1 wt % total surfactant (15 mol % BTHA and 85 mol % SDS) in D_2O, after equilibration for 1 day in the dark at 25 °C. Plotted above the experimental data is a line corresponding to a slope of −2, which is indicative of a bilayer geometry according to Guinier analysis (eq 4). Inspection of Figure 3A reveals that while the experimental data generally follows a slope of −2, it also contains a slight oscillatory component with a weak maximum at $q = 0.02$ Å^{-1}. Figure 3B shows the SANS data for the trans sample when fit with the polydisperse core−shell model. From the fit, we obtain a mean core radius of 330 Å, a bilayer thickness of 28 ± 0.2 Å, and a polydispersity of 0.308. The core radius obtained from this model is somewhat smaller than that obtained by QLS (675 Å), but this is likely due to the fact that QLS is strongly biased toward larger objects in solution.[29] Past studies have demonstrated that SANS from populations of vesicles with low size polydispersity is characterized by an oscillation in $I(q)$ caused by the form factor of such a population of vesicles.[12,13] In contrast, a polydisperse population of vesicles exhibits a scattering curve that does not contain an oscillatory component and conforms closely to the Guinier prediction.[13] The results in Figure 3 thus suggest that vesicles formed by mixtures of *trans*-BTHA and SDS may have a narrower polydispersity than vesicles formed, for example, from mixtures CTAB and SOS.[13]

Figure 4 shows the IFT results for the trans sample obtained from the data in Figure 3A. The pair distance distribution function, $p(r)$, is shown in Figure 4A. The curve has a broad, symmetric shape, that, when compared with Figure 2 (dashed line), reveals that the $p(r)$ for mixtures of *trans*-BTHA and SDS resembles that of vesicles. The value of r where $p(r)$ decays to 0 indicates the size of the aggregate. From Figure 4A, we estimate a maximum size of 1400 Å, which agrees well with the value obtained from QLS (see Table 1).

Next we determined the thickness pair distance distribution function, $p_t(r)$, of the bilayer of the vesicle by using data in Figure 3A corresponding to $q > 0.03$ Å^{-1}. Limiting the data to high q in this IFT analysis isolates the scattering from the bilayer of the vesicle. The bilayer thickness of the vesicle is determined by the value of r at which the $p_t(r)$ function becomes zero. Figure 4B shows the $p_t(r)$ calculated for the trans sample. Inspection of Figure 4B shows that the bilayer thickness of the trans sample is 35 ± 2 Å, in good agreement with the end-to-

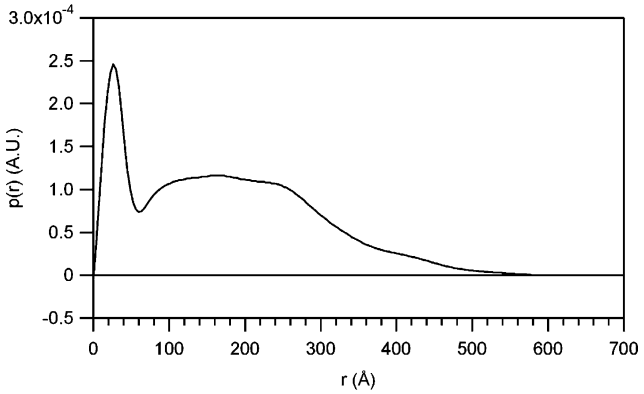

Figure 5. Pair distance distribution function, $p(r)$, obtained by IFT analysis of the cis-rich BTHA/SDS sample shown in Figure 3A.

end length of a fully extended BTHA molecule (33 Å). The bilayer thickness can also be estimated by plotting $[p(r)/r]$. For vesicles, at small r values $p(r)$ scales with r^2 and then changes to a linear dependence on r at a value of r corresponding to the bilayer thickness ("T" in Figure 2). As shown in Figure 4C, by locating the crossover (marked with an arrow), we estimate a bilayer thickness of approximately 35 Å. This value is in good agreement with the value obtained by calculating $p_t(r)$. These results suggest that BTHA likely spans the bilayer. Because the rigid *trans*-azobenzene group imparts steric constraints on the conformation of the molecule, it seems unlikely that BTHA would form a "looped" conformation in which the two headgroups of BTHA reside on the same side of the bilayer.

Cis-Rich Sample. Next, we illuminated solutions of *trans*-BTHA and SDS with UV light to prepare solutions that were rich in the cis isomer of BTHA. For solutions containing 0.1 wt % total surfactant (15 mol % BTHA/85 mol % SDS), we determined from UV−vis measurements that the photostationary state under the conditions of illumination used in our study corresponded to approximately 80% cis isomers of BTHA. We note here that isomerization of the solution is accompanied by a change in the color from pale yellow (as noted above) to orange.

We first used QLS to characterize the cis-rich solution shortly after the photostationary state under UV illumination had been achieved. Because the cis isomer thermally relaxes over a period of 12 h in the absence of UV light, we continuously illuminated the cis sample during both QLS and SANS experiments. Inspection of Table 1 shows that the intensity-average hydrodynamic size of the aggregates in the cis-rich solution was 240 ± 50 Å. We also note that the intensity of light scattered from these solutions decreased from 160 kcps to 1.4 kcps upon photoisomerization of the *trans*-BTHA/SDS mixture to the photostationary state. As depicted in Figure 3A, the SANS data for the cis-rich sample follows a −1 slope at low q values, which suggests a cylindrical geometry according to Guinier theory (eq 3). Figure 5 shows the $p(r)$ obtained from an IFT analysis of the scattering data obtained from the cis-rich sample. Two peaks are evident, a sharp peak at approximately r = 25 Å and a broader peak centered at about r = 160 Å, followed by a decay to 0. At small r values, $p(r)$ for a cylinder increases with r^2 (Figure 2). At a threshold value of $r = 2R_c$, where R_c is the radius of the cross section of the cylinder, $p(r)$ for a rigid cylinder changes from the r^2 dependence to a linear dependence, reflecting correlations along the length of the cylinder. For rigid cylinders, the point where $p(r)$ decays to 0 indicates the length of the cylinder (400 Å in Figure 2). $2R_c$ can be determined from the point of inflection in the $p(r)$.[10] From the data in Figure 5 we calculate a cross-sectional radius of 19 ± 3 Å, which is close to half the length of a BTHA molecule (17 Å) or a fully extended SDS chain (17 Å). For $r > 2R_c$, we do not observe the linear decay of the $p(r)$ function, as expected for a rigid cylinder. Instead, we see a broad peak centered at about r = 160 Å followed by a decay of the $p(r)$ to 0. Such a peak could arise from interactions between cylindrical aggregates [i.e., for $S(q) \neq 1$]. Alternatively, if the cylinders are not rigid, then the second peak could reflect the flexibility of the aggregates.

Trans Sample After Photocycle. As described above, cis-rich samples, when left in the dark at 25 °C, relax over a period of hours to trans isomers in the absence of UV illumination. Following thermal relaxation of a solution of cis-rich BTHA and SDS to a solution of *trans*-BTHA and SDS, we sought to determine if the microstructure of the solution corresponded to vesicles of the type seen upon mixing *trans*-BTHA and SDS initially. After collecting SANS data for the cis-rich sample, the cell holder and sample were equilibrated in the dark for 18 h before acquisition of a second SANS spectrum. This sample is designated as *TCT* (for trans → cis → trans). We also performed UV−vis measurements of these thermally relaxed samples to confirm the presence of the trans isomers in the sample. The UV−vis spectrum of the *TCT* sample overlapped that of the initial trans sample (data not shown), indicating that relaxation of the BTHA to the trans state was complete after 18 h of equilibration in the dark. Measurements obtained using QLS (Table 1) reveal that the *TCT* samples contain aggregates with average hydrodynamic diameters that are indistinguishable (within experimental error) from the aggregates in the initial trans sample. This holds true for samples prepared in both D_2O and H_2O.

Figure 3A shows the SANS spectra (scaled by a factor of 10 for clarity), and Figure 6 shows the IFT results for the *TCT* sample. The overlap of unscaled SANS data for the trans sample and the *TCT* sample is excellent, except for an oscillation in the range 0.008 Å < q < 0.015 Å. As discussed above, this oscillation may indicate that the distribution of aggregates in the *TCT* sample has a low polydispersity. Figure 3B shows the results from fitting the *TCT* data with the polydisperse core−shell model. We obtain a core radius of 430 Å, a thickness of 28 ± 0.2 Å, and a polydispersity of 0.184. The lower polydispersity as compared to that of the trans confirms that the oscillations in the data result from the distribution of sizes, as the core radius and bilayer thickness compare well with the trans sample. Inspection of the $p(r)$ obtained for the *TCT* sample (Figure 6A) reveals that it resembles that of the trans sample before illumination. Although $p(r)$ for the *TCT* sample is less symmetric than that for the trans sample prior to illumination, the $p_t(r)$ for the *TCT* sample (Figure 6B) and the plot of $p(r)/r$ (Figure 6C) are similar to those for the trans sample. These plots yield a bilayer thickness of 34 ± 2 Å. These results, when combined, lead us to conclude that the state of aggregation of the *TCT* sample corresponds to vesicles.

Comparison to Other Surfactant Systems. Vesicles have been shown to form in a variety of mixed cationic and anionic surfactant systems. Most of the systems reported to date employ surfactants with one ionic headgroup (classical surfactant architecture). Our results suggest that rigid, bolaform surfactants can also form vesicles in which the bolaform surfactants likely span the bilayer and, thus, dictate the bilayer thickness of the vesicle. In contrast, classical cationic/anionic systems form

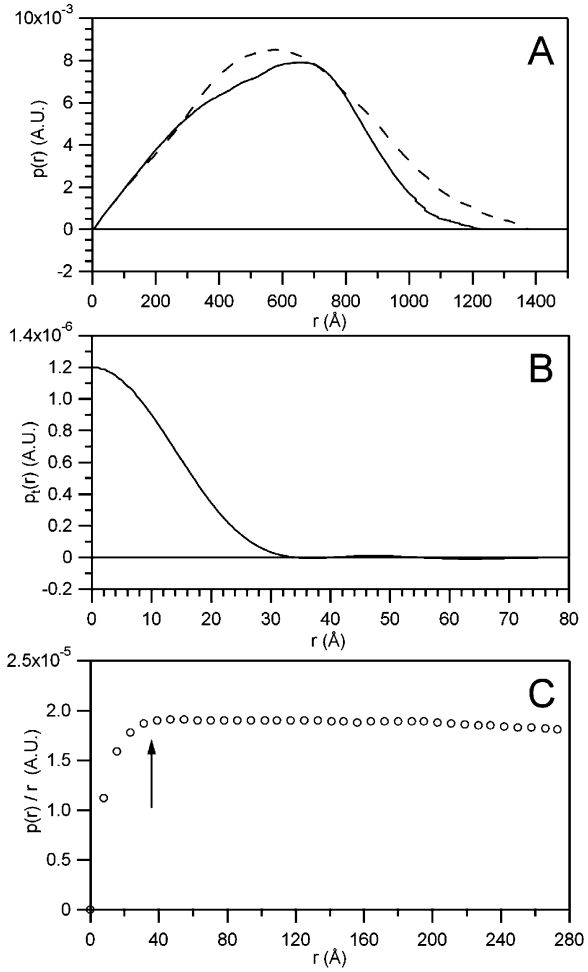

Figure 6. (A) Pair distance distribution function for the *trans*-BTHA/SDS sample after a photocycle, as calculated from the data shown in Figure 3A (solid line). Also plotted is the $p(r)$ for the trans-BTHA/SDS sample (dashed line). (B) Thickness pair distance distribution function and (C) a plot of $p(r)/r$ vs r for the *trans*-BTHA/SDS sample after a photocycle. The arrow marks the crossover in $p(r)$ from r^2 to linear dependence.

vesicles with bilayer thicknesses that depend on several factors related to the packing of the surfactants, for example, tail length asymmetry or the size of headgroups.[5,10,25] We also note here that use of a rigid bolaform surfactant constrains the vesicle to have an equal number of cationic groups in each leaf of the bilayer of the vesicle, which is not the case for systems with single headgroups. We speculate that these packing constraints may cause vesicles formed by rigid, bolaform surfactants to be stabilized by spontaneous curvature rather than entropic effects. Past studies have demonstrated that this mechanism of stabilization leads to a size distribution that is narrower than entropically stabilized systems such as that formed by CTAB and SOS. We observed oscillations in SANS spectra of samples containing BTHA and SDS (see Figure 3), which is consistent with a population of vesicles with a narrow size distribution. The *TCT* sample is particularly interesting in that vesicles are formed without external shearing or mixing, as is common during the preparation of vesicles from other surfactant systems.

Here we also briefly compare the results of our study to those of past studies of azobenzene and stilbene-based surfactants.[22,34] First, we mention the work of Eastoe and co-workers who studied mixtures of cationic surfactants containing stilbene. These authors report a vesicle-to-micelle transition induced by illumination with UV light (254 nm). This transition was not completely reversible due to cyclization and dimerization reactions that accompany illumination of the stilbene surfactants with UV light. In a separate work, Sakai and co-workers synthesized an azobenzene surfactant with a single cationic headgroup[22] and studied mixtures of that surfactant, AZTMA, with SDBS. Using freeze-fracture cryo-transmission electron microscopy, they determined that mixtures of *trans*-AZTMA and SDBS (0.05 wt % total surfactant, molar ratio 6:4 AZTMA/SDBS) form a phase containing vesicles and lamellae, with vesicles that range in size from 500 to 1000 Å. We point out several differences between their observations obtained using AZTMA and SDBS and measurements reported in this paper using BTHA and SDS. First, whereas AZTMA and SDBS formed phases containing mixtures of vesicles and lamellae, we observed BTHA and SDS to form phases containing vesicles in the absence of coexisting lamellae. Second, mixtures of AZTMA and SDBS were observed to precipitate upon illumination with UV light, whereas mixtures of BTHA and SDS reported in this paper form cylindrical microstructures without formation of precipitate. Whether or not these differences in behavior reflect the architecture of the surfactants or the locations of the surfactant mixtures in their respective phase diagrams (measurements reported in this paper correspond to the SDS-rich side of the phase diagram whereas measurements reported with AZTMA and SDBS correspond to the AZTMA-rich side of the phase diagram) remains to be determined. We are currently measuring the phase diagram for the BTHA/SDS/H_2O system and will report these measurements in a future publication.

Conclusion

We have used SANS to demonstrate that mixtures of a light-sensitive, cationic surfactant (BTHA) and an anionic surfactant (SDS) spontaneously form vesicles in aqueous solution. The SANS measurements indicate the thickness of the bilayer of the vesicles to be 35 ± 2 Å, consistent with a conformation of the rigid BTHA molecule in which it spans the bilayer. This observation suggests an approach to control the bilayer thickness of vesicles. Illumination of a mixture of *trans*-BTHA and SDS in H_2O or D_2O with UV light transformed the vesicles into smaller cylindrical aggregates. Thermal relaxation of the cis-rich solution of BTHA and SDS back to a *trans*-rich state resulted in the recovery of the vesicles. SANS of the vesicles formed by BTHA and SDS suggests a distribution of sizes that is narrower than vesicles formed by CTAB and SOS, consistent with a model in which steric constraints imposed by a rigid, bolaform architecture influence the aggregation behavior of this surfactant system. Finally, these results demonstrate that mixed cationic/anionic surfactant systems can form the basis of complex fluids with microstructures and properties that can be tuned by illumination with light.

Acknowledgment. We acknowledge the support of the National Institute of Standards and Technology, U.S. Department of Commerce, in providing the neutron facilities used in this work. This work utilized facilities supported in part by the National Science Foundation under Agreement No. DMR-9986442. N.L.A. also acknowledges support from CTS-0327489.

LA050263C

(34) Eastoe, J.; Dominguez, M. S.; Wyatt, P.; Orr-Ewing, A. J.; Heenan, R. K. *Langmuir* **2004**, *20*, 6120−6126.